***Date**: February 1, 2024*
Department of Translational Molecular Pathology (TMP)
Immune Profiling Laboratory
Cancer Immune Monitoring and Analysis Center
The University of Texas MD Anderson Cancer Center
TMP-Immunoprofiling (TMP-IL) Laboratory Director:
Cara Haymaker, Associate Professor, TMP
Immunohistochemistry and Digital Pathology Lab Director:
Luisa Maren Solis Soto, Associate Professor, TMP

THE UNIVERSITY OF TEXAS MD Anderson Cancer Center
Making Cancer History®

Analytical Validation of RNAscope Assay for Immuno-oncology Biomarker Probes

1. Technical platform

The RNAscope® Assay uses *in situ* hybridization (ISH) to visualize single RNA molecules per cell in formalin-fixed, paraffin-embedded (FFPE) tissue mounted on slides. The tissue section is pretreated with heat and enzyme, then hybridized with RNA-specific probes to target RNAs. The signal is then amplified using multiple steps, followed by hybridization to horseradish peroxidase (HRP)-labeled probes and detected using the 3,3'-diaminobenzidine (DAB) chromogenic substrate. Each single RNA transcript will appear as a distinct dot of chromogen precipitate that is visible using a common brightfield microscope(1, 2).

This document describes **verification and validation of the assay performance** of different RNAscope probes that have been performed at the Translational Molecular Pathology Immunoprofiling Laboratory (TMP-IL). Assay conditions that have been optimized for tonsil tissue and solid tumors (lung cancer tissue) are presented in this report. Optimal tissue pretreatment conditions of target retrieval and/or protease digestion have been reached using negative (*DapB*, dihydrodipicolinate reductase gene from the *Bacillus subtilis*) and positive control probe (*PPIB*, peptidylprolyl Isomerase B)(for medium expression level genes) to obtain the best signal and cell morphology features. For any new cohort to be tested, a verification step using *PPIB* is performed. When *PPIB* signals are low, adjustments of pretreatments conditions can be made using *PPIB* probes, to obtain the highest positive control signal per tissue type. Alternatively, for low expression targets (3-15 copies per cells), probes that target *Polr2A (*DNA-directed RNA polymerase II subunit A) can be used instead of *PPIB* probe*.* For high expression targets (>20 copies per cell), a probe that target *UBC* (Ubiquitin C) can also be used.

2. Analytes

a) RNAscope probes:
- ✓ Target probes: *CTLA4, CD274* (PD-L1), *IL10, IFNG*, *TNFRSF8* (CD30)
  - RNAscope® LS 2.5 Probe- Hs-CTLA4: Cat# 554348
  - RNAscope® LS 2.5 Probe- Hs-CD274 (PD-L1): Cat# 600868
  - RNAscope® LS 2.5 Probe- Hs-IL-10: Cat# 602058
  - RNAscope® LS 2.5 Probe- Hs-IFNG: Cat# 310508
  - RNAscope® LS 2.5 Probe- Hs-TNFRSF8 (CD30): Cat # 593458
- ✓ Control probes: *PPIB*, *DapB*.
  - RNAscope® 2.5 LS Positive Control Probe – Hs-PPIB (Cat# 313908)
  - RNAscope® 2.5 LS Negative Control Probe – DapB (Cat# 312038)

b) Reagents, controls, and calibrators

Reagents

- ✓ RNAscope 2.5 LSx Reagent Kit – Brown (Cat# 322700)
    - RNAscope 2.5 LSx Rinse
    - RNAscope 2.5 LSx Hematoxylin
    - RNAscope 2.5 LSx DAB
    - RNAscope 2.5 LSx Bluing
    - RNAscope 2.5 LSx AMP 1 DAB
    - RNAscope 2.5 LSx AMP 2 DAB
    - RNAscope 2.5 LSx AMP 3 DAB
    - RNAscope 2.5 LSx AMP 4 DAB
    - RNAscope 2.5 LSx AMP 5 DAB
    - RNAscope 2.5 LSx AMP 6 DAB
    - RNAscope 2.5 LSx H_2O_2
    - RNAscope 2.5 LSx Protease
- ✓ Leica BOND Reagents
    - BOND Epitope Retrieval Solution 2-1L (RTU) (Cat# AR9640)
    - BOND Dewax Solution – 1L (RTU) (Cat# AR9222)
    - BOND Wash Solution 10X Concentrate – 1L (Cat# AR9590)

Equipment:

- ✓ BOND RX Fully Automated Research Stainer from Leica Biosystems

Control slides:

- ✓ RNAscope® Control Slides - Human HeLa Cell Pellet (Cat# 310045)

3. Scoring and RNA quality control

Evaluation of RNA signals using standard microscopy. A semi-quantitation scoring system was applied in a scale of 0 to 4+, based on the number of RNA copies per cell following Advanced Cell Diagnostics (ACDbio) Guidelines **Table 1**:

Table 1. Advanced Cell Diagnostics Scoring Guidelines

Score	RNA ISH score (ACDbio Scoring Criteria)
0	No staining or <1 dot/ 10 cells
1+	1-3 dots/cell
2+	4-9 dots/cell. None or very few dot clusters
3+	10-15 dots/cell and <10% dots are in clusters
4+	>15 dots/cell and >10% dots are in clusters

All probes (targets, and control probes, *PPIB* and *DapB* probes) were scored using conventional bright-field microscopy. The samples with a *DapB* (negative control) score of <1+ and a *PPIB* (positive control) score ≥2+ with relatively uniform *PPIB* signals throughout the tissue, were considered adequate for analysis.

For target probes, RNA signals were also quantified and scored by digital image analysis with HALO software v3.5.3577, Indica Labs, Inc. using algorithm settings ISH v4.1.3 and creating annotation settings with target probe markup. The cell scoring for the target probe was set following ACDbio Scoring Guidelines **Table 1**. The results were reported as total tissue area (μm^2), total copies of target probe, total area of target probe (μm^2), average positive optical density (AOD) of target probe and average copies per μm^2 of target probe.

Probes for *CD274* (PD-L1) in lung cancer tissue placed in a tissue microarray was previously evaluated using an H-score (0-400) in malignant cells obtained by digital image analysis (Aperio, Leica biosystem) using the Aperio RNA ISH Algorithm.

In immune-oncology research, both methods, standard microscopy and/or digital image analysis, can be used to quantitate RNA signals. Standard microscopy is recommended to evaluate positive and negative control probes. Digital image analysis of RNA target probe can provide a more objective assessment of *in situ* RNA expression.

4. Analytical characteristics

Table 2. Analytical characteristics of validation of RNAscope assay.

RNAscope assay using single chromogen	
Parameters	mRNA signals obtained by RNAscope assays are visualized using brown chromogen (DAB) evaluated by standard microscopy and categorized as 0, 1+, 2+ 3+, 4+, using the ACDbio score system. Positive expression was defined as score >=1+, negative expression was defined as score 0. Digital image analysis was also performed in annotated regions, average positive optical density (AOD) and H-score (0-300) of target probe were used for this report. H-score >10 was considered positive. **Section 3; Table 1, and Section 5.**
Accuracy	Accuracy was measured by the capacity of the assay to accurately identify positive cells for immune biomarker probes in reactive tonsil tissue with a pattern of expression concordant with biological expression [genes that are expressed by immune cells are expected to have positive/high expression in immune cells from the interfollicular area (IA), germinal center (GC), or reticulated epithelium (RE), compared to fibroconnective tissue]. Using *CTLA4, CD274 (PD-L1), IL10, IFNG, and TNFRSF8* (CD30) probes and the ACDBio score system (0-4+) we found that immune cells had scores >=3+, while non-immune cells have score 0 (negative expression) for all probes in tonsil tissue. **Section 6; Table 3; Figure 1.** Quantitative analysis of these target probes showed that the AOD was lower in immune-scarce fibroconnective tissue compared to immune cell-enriched compartments (GC, IA, and RE), this difference was statistically significant (*P*<0.001) for CTLA*4, CD274* (PD-L1), *IL10, and TNFRSF8 (CD30)*. For *IFNG,* AOD in fibroconnective tissue was lower than other compartments but did not reach statistical significance. **Section 6; Table 5, 6 and 7; Figure 1 and 2.** To better assess the accuracy of RNAscope signals, we compared the AOD of *CD274, CTLA4* and *TNFRSF8* probes with their corresponding protein expression patterns (AOD) using immunohistochemistry (IHC). Correlation between scores obtained by RNAscope and IHC were positive for all of them. The correlation was statistically significant (*P*<0.005) for *CD274* (PD-L1) (Spearman r, 0.7008) and *TNFRSF8* (CD30) (Spearman r, 0.4638), while for *CTLA4* (CTLA4) the correlation was low (r=0.2512) and did not reach statistical significance. **Section 6; Figure 1 and 3**
Analytical sensitivity	Analytical sensitivity was measured by the capacity of the assay to identify true positive expression as defined by gene amplification or by protein expression. We compared biomarker expression of a lung cancer TMA by RNAscope assay with the gene copy number by FISH and with the protein expression by standard IHC. Using *CD274* gene amplification as gold standard, we found that the assay has a sensitivity of 81%. Using protein PD-L1 IHC assay as gold standard the assay has a sensitivity of 73%. **Section 7; Table 8 and 9; Figure 4.**
Analytical specificity	Analytical specificity was measured by the capacity of the assay to identify true negative expression as defined by gene amplification or by protein expression. We compared biomarker expression of a lung cancer TMA by RNAscope assay with the gene copy number by FISH and with the protein expression by standard IHC. Using *CD274* gene

	amplification as gold standard, we found that the assay has a specificity of 68%. Using protein PD-L1 IHC assay as gold standard the assay has a specificity of 77%. **Section 7; Table 8 and 9; Figure 4.**
Precision Intra and Inter-assay reproducibility	Inter-assay reproducibility was measured by testing three different runs, on different days. Intra-assay reproducibility was measured by testing 2 different assays on the same day and at the same run. The AOD of RNAscope signals in all the selected biological compartments was used to correlate the reproducibility of *TNFRSF8* target probe signals in inter and intra-run tests. Inter-assay tests showed positive correlation (Spearman r, 0.84, *P*<0.001) of AOD of *TNFRSF8* RNAscope probe measured in serial sections of a tonsil tissue run at different days (Day 1 and Day 7). Intra-assay tests showed positive correlation (Spearman r, 0.71, P<0.001) of AOD of *TNFRSF8* RNAscope probe measured in serial sections of a tonsil tissue in the same run (Day7). **Section 8; Figure 5 and 6.**
Establishment of appropriate quality control & improvement procedures	Positive and negative control probes are performed for every test. All the required equipment has annual service contracts with regular Preventive Maintenance performed to maintain optimal calibration and performance. All other small equipment and laboratory material have calibration performed by certified vendors. No external validation was performed.

5. Analytical data

mRNA signals obtained by RNAscope assays are visualized using brown chromogen (DAB) evaluated by standard microscopy and categorized as 0, 1+, 2+ 3+, 4+. Digital image analysis was also performed in annotated regions, average positive optical density (AOD) and H-score of target probe were used for this report.

Samples: Formalin-fixed paraffin embedded (FFPE) Tonsil tissue (11 sections), FFPE lung cancer (non-small cell lung carcinoma, NSCLC) whole section tissue (3 samples, 15 sections), FFPE NSCLC placed in a Tissue microarray (TMA) (n=193 tumor tissue) (1mm width core) **Table 3.**

Scoring: The RNAScope stained slides of different immune targets were evaluated by a pathologist using both standard microscopy and digital image analysis.

Standard Microscopy evaluation: The analysis using standard microscopy included presence and patterns of mRNA transcripts displayed as single dots or in clusters (with absence of non-specific background), cellular pattern of expression (immune cells vs. non-immune cells) and patterns of expression in different biological compartments of a tonsil tissue. The biological compartments were categorized as **immune cell-enriched compartments** (germinal center, interfollicular area, and reticulated epithelium) and **immune cell-scarce compartment** (fibroconnective tissue with low or absence of immune cells).

Table 3. Evaluation of RNAscope stained slides of different target probes using standard brightfield microscopy.

Analyte	Date	Tissue tested	Score in immune cells	Score in non-immune cells	Cellular pattern of expression	Nonspecific Background
CTLA4						
	1/2/2018	Tonsil	4+	0	Positive in immune cells in GC, IA, RE; Negative in fibroconnective tissue	Absent
	1/22/2018	Lung cancer c.922	3+	0	Positive in immune cells; negative in epithelial malignant cells	Absent
	1/2/2018	Lung cancer c.945	2+	0	Positive in immune cells; negative in epithelial malignant cells	Absent
	1/22/2018	Lung cancer c.157	3+	0	Positive in immune cells; negative in epithelial malignant cells	Absent

CD274 (PD-L1)						
	1/30/2017	Tonsil	3+	1+	Positive in immune cells and in isolated epithelial cells; negative in fibroconnective tissue	Absent
	1/30/2017	Lung Cancer TMA (n=193)	3+	1+	Positive in immune cells and in some tumor cells	Present in few tumor cells
IL10						
	1/2/2018	Tonsil	4+	0	Positive in immune cells in GC, IA, RE; Negative in fibroconnective tissue	Absent
	1/22/2018	Lung cancer c.922	0	0	Negative in immune cells and epithelial malignant cells	Present in few tumor cells
	1/22/2018	Lung cancer c.945	0	0	Negative in immune cells and epithelial malignant cells	Absent
	1/22/2018	Lung cancer c.152	1+	0	Positive in immune cells; negative in epithelial malignant cells	Absent
IFNG						
	1/2/2018	Tonsil	3+	0	Positive in immune cells in GC, IA, RE; Negative in fibroconnective tissue	Absent
	1/22/2018	Lung cancer c.922	0	0	Negative in immune cells and epithelial malignant cells	Absent
	1/22/2018	Lung cancer c.945	0	0	Negative in immune cells and epithelial malignant cells	Present in isolated immune cells
	1/22/2018	Lung cancer c.152	1+	0	Positive in immune cells; negative in epithelial malignant cells	Absent
TNFRSF8						
	9/7/2022	Tonsil	4+	0	Positive in immune cells in GC, IA, RE; Negative in fibroconnective tissue	Absent
	11/29/2023	Tonsil (T51-2) Test1	4+	0	Positive in immune cells in GC, IA, RE; Negative in fibroconnective tissue	Absent
	12/5/2023	Tonsil (T51-2) Test2_1	4+	0	Positive in immune cells in GC, IA, RE; Negative in fibroconnective tissue	Absent
	12/5/2023	Tonsil (T51-2) Test2_2	4+	0	Positive in immune cells in GC, IA, RE; Negative in fibroconnective tissue	Absent
DapB						
	1/2/2018	Tonsil	0	0	Negative in immune cells and epithelial malignant cells	Absent
	1/2/2018	Lung cancer c.922	0	0	Negative in immune cells and epithelial malignant cells	Absent
	1/2/2018	Lung cancer c.945	0	0	Negative in immune cells and epithelial malignant cells	Absent
	1/2/2018	Lung cancer c.152	0	0	Negative in immune cells and epithelial malignant cells	Absent
PPIB						
	1/2/2018	Tonsil	>=2+	>=2+	Positive in most cells	Absent
	1/2/2018	Lung cancer c.922	>=2+	>=2+	Positive in most cells	Absent
	1/2/2018	Lung cancer c.945	>=2+	>=2+	Positive in most cells	Absent
	1/2/2018	Lung cancer c.152	>=2+	>=2+	Positive in most cells	Absent
	1/2/2018	Hela	4+	4+	Positive in most cells	Absent
	9/2/2022	Hela	4+	4+	Positive in most cells	Absent
	8/30/2022	Hela	4+	4+	Positive in most cells	Absent
	7/27/2022	Hela	4+	4+	Positive in most cells	Absent
	7/28/2022	Hela	4+	4+	Positive in most cells	Absent
	11/29/2023	Tonsil	4+	4+	Positive in most cells	Absent
	11/29/2023	Hela	4+	4+	Positive in most cells	Absent

Notes: GC, germinal center; IA, Interfollicular area; RE, reticulated epithelium; FT, fibroconnective tissue.

Digital Image analysis: The RNAscope slides of tonsil tissues were scanned at 40x using Aperio AT2 (Leica Biosystem) applying Z-stack settings. Subsequently, they were visualized using Halo software (algorithm settings ISH v.4.1.3). A total of 40 regions of interest (ROIs) in different biological compartments were randomly selected, namely germinal center, interfollicular area, reticulated epithelium and fibroconnective tissue (10 ROIs in each compartment). In RNAscope stained images, the target probe was identified as brown dots, each dot representing a single RNA molecule per cell. Using the ISH v4.1.3 algorithm, a probe markup was established to identify and quantify the target probe in the selected ROIs. The outputs evaluated for each biological compartment included total tissue area (μm^2), total copies of target probe, total area of target probe (μm^2), AOD of target probe and average copies per μm^2 of target probe.

Annotated data: The lung carcinoma TMA containing 193 non-small cell lung carcinoma tumor tissue samples stained with RNAscope for *CD274* was previously analyzed. *CD274* (PD-L1) RNA expression was evaluated using an H-score (0-300) in malignant cells obtained by digital image analysis (Aperio, Leica biosystem) using the Aperio RNA ISH Algorithm, in this analysis, the expression of each cell was categorized as 0 (<1 dot/ cell);

1+ (1-5 dots per cell); 2+ (6-20 dots per cell), 3+ (21 or more dots per cell). In the lung carcinoma TMA, annotated information of percentage of protein PD-L1 expression in malignant cells by IHC (PD-L1, clone E1L3N, cell signaling) and gene copy number by Fluorescence *in situ* Hybridization (FISH) (*CD274,* ZytoLight SPEC CD274,PDCD1LG2/CEN9 Dual Color FISH Probe (PL138)) were available for all samples. PD-L1 was categorized as: PD-L1 positive by IHC,>=1% of expression in the membrane in malignant cells; *CD274* positive by RNAscope, >10 H-score (at least 10% of malignant cells with >=1 dot per cell); *CD274* positive by FISH: >=6 gene copy number in malignant cells

Immunohistochemistry (IHC) analysis: To compare the expression of different targets with corresponding protein expression, IHC was also performed for the following biomarkers: PD-L1, CTLA4 and CD30.

Antibody clones and conditions are provided in **Table 4.**

Table 4. Clones and conditions used for immunohistochemistry evaluation.

Antibody	Clone	Vendor	Dilution	Antigen Retrieval
PD-L1	E1L3N	CST	1:200	pH9
CD30	Ber-H2	DAKO	1:50	pH6
CTLA-4	BSB-88	BioSB	1:100	pH9

6. Accuracy

To assess accuracy, we evaluated if the assay could correctly identify RNAscope signals in reactive tonsil tissue with a pattern of expression concordant with biological expression. Genes that are expressed by immune cells such as *CTLA4, CD274* (PD-L1), *IL10, IFNG*, *TNFRSF8* (CD30) are expected to have positive/high expression in immune cells from the interfollicular area (IA), germinal center (GC), or reticulated epithelium (RE), compared to fibroconnective tissue (FT). In addition, we compared the expression of target probes with orthogonal IHC assay.

Evaluation of expression patterns of immune biomarkers in tonsil tissue and whole section of lung cancer tissue using RNAscope assay

We used tonsil tissue stained with *CTLA4, CD274* (PD-L1), *IL10, IFNG*, and *TNFRSF8* (CD30) probes by RNAscope assay . A pathologist evaluated RNAscope expression using standard microscopy and ACDbio Score system in immune cells and non-immune cells (fibroblast or epithelial cells). In Tonsil tissue all target probes displayed various levels of expression in different biological compartments, scores were >=3+ in immune cells while non-immune cells have negative (score 0) expression for *CTLA4, IL10, IFNG, TNFRSF8* (CD30) probes. *For CD274 the* score in non-immune cell was of 1+, and positive expression was observed in the reticulated epithelium while other non-immune cells where negative (0). These findings are concordant with biological expected expression. **Table 3**

To evaluate the pattern of expression of immune probes in carcinoma tissue we used whole section non-small cell lung carcinoma stained with *CTLA4, IL10, IFNG*, and *TNFRSF8* (CD30) probes, ACDbio scores varied from 0 to 3+ in immune cells, while non-immune cells were negative (0) for all NSCLC samples (n=3) for all probes. These findings highlight the heterogeneity of expression of immune probes in carcinoma tissue.

Quantitative analysis of target RNA probes and comparison with immunohistochemistry using digital image analysis

In addition, we performed a quantitative analysis of these targets in different tonsil compartment using digital image analysis. We used the AOD of RNAScope signals to evaluate differential gene expression among them. For *CD274* (PD-L1), *CTLA4, IL10, IFNG, TNFRSF8* (CD30) probes, the median of AOD was lower than 0.285 (0.2381-0.2843) in fibroconnective tissue, and higher than 0.285 in GC, IA and RE (range 0.2871-0.5933).

CTLA4, CD274 (PD-L1), *IL10,* and *TNFRSF8* (CD30) have higher levels of expression in immune cell-enriched compartments (GC, IA, RE) compared to immune-scarce fibroconnective tissue (P<0.05) as shown in **Table 5 and Table 6.** *IFNG* levels of expression measured by AOD of RNAscope signal was lower in fibroconnective tissue, but this difference did not reach statistical significance. Descriptive statistics of this analysis is provided in **Table 7.**

Importantly *CD274* expression was significantly higher in the reticulated epithelium compared to other compartments which is concordant with protein expression patterns, and the immunosuppressive role of PD-L1 in crypts of tonsil tissue (3-5). *TNFRSF8* expression was significantly higher in the germinal center compared to other compartments which is also concordant with protein expression pattern of CD30 expression in immunoblasts which are located in the germinal centers(6, 7).

Table 5. Median Average Positive Optical Density of RNAscope signal of *CD274* (PD-L1), *CTLA4, TNFRSF8* (CD30), *IFNG*, and *IL10* probes in different biological compartments of tonsil tissue.

Probes	Median Average Positive Optical Density			
	Germinal Center	**Interfollicular Area**	**Reticulated Epithelium**	**Fibroconnective Tissue**
CD274	0.3282	0.3510	0.4004	0.2381
CTLA-4	0.4635	0.5665	0.5933	0.2496
TNFRSF8	0.4278	0.3713	0.353	0.2688
IFNG	0.3412	0.2871	0.3486	0.2292
IL-10	0.4597	0.4668	0.5026	0.2843

Table 6. Multiple comparisons of RNAscope signals of *CD274* (PD-L1), *CTLA4, TNFRSF8* (CD30), *IFNG*, and *IL10* probes in different tonsil tissue compartments.

			Adjusted *P* value				
Comparison	**n1**	**n2**	***CD274***	***CTLA4***	***TNFRSF8***	***IFNG***	***IL10***
GC vs. FT	10	10	0.0019	<0.0001	<0.0001	0.0593	<0.0001
IA vs. FT	10	10	<0.0001	<0.0001	<0.0001	0.6871	<0.0001
RE vs. FT	10	10	<0.0001	<0.0001	<0.0001	0.0522	<0.0001
GC vs. IA	10	10	0.7352	0.0375	0.0122	0.7204	0.7553
GC vs. RE	10	10	0.0022	0.0009	0.0066	>0.9999	0.2502
IA vs. RE	10	10	0.0328	0.509	0.9955	0.6871	0.8055

Notes: GC, germinal center; IA, Interfollicular area; RE, reticulated epithelium; FT fibroconnective tissue

Quantitative analysis of target RNA probes and comparison with immunohistochemistry using digital image analysis

To better assess the accuracy of RNAscope signals, we compared the RNAscope signals of *CD274, CTLA4* and *TNFRSF8* genes with the protein expression patterns using IHC, **Figure 1 and 2**. In both assays, the stained slides were scanned at 40x and evaluated using HALO software, with the ISH v4.1.3 algorithm for RNAscope and Area Quantification v2.4.2 algorithm for IHC. For both assays, a probe markup was established to identify and quantify the target probe in the selected ROIs. The outputs evaluated for RNAscope in each selected biological compartment included total tissue area (μm^2), total copies of target probe, total area of target probe (μm^2), AOD of target probe and average copies per μm^2 of target probe. For IHC, the evaluated outputs included

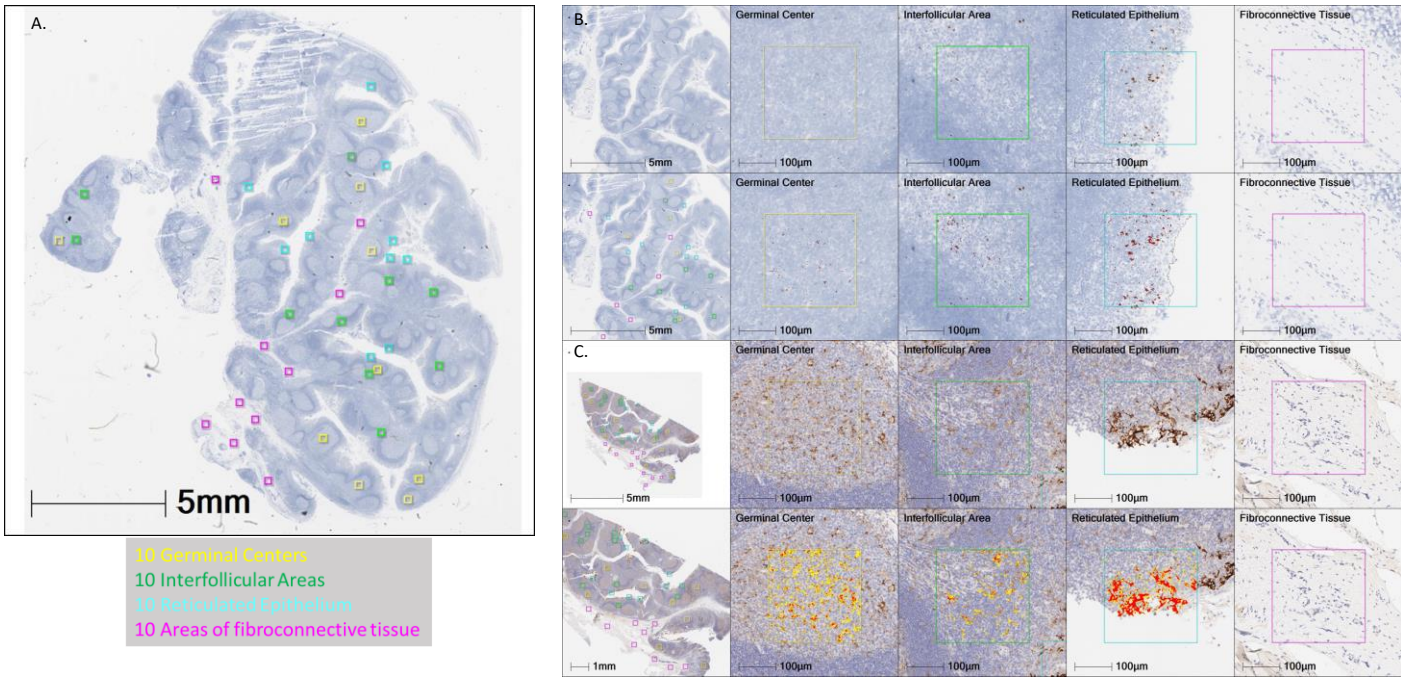

Figure 1. Digital image analysis of *CD274* (PD-L1) with RNAscope and Immunohistochemistry. A) Microphotographs of FFPE tonsil tissue illustrating the ROIs selected in different biological compartments of RNAscope evaluation. B&C) Microphotographs of FFPE tonsil tissue illustrating digital image analysis of *CD274* (PD-L1) RNAscope ISH staining and immunohistochemistry in different biological compartments. B) Upper row shows RNAscope ISH staining of PD-L1 target probe as brown dots (each dot represents a single RNA molecule); lower row shows the probe mark-up identifying PD-L1 target probe. C) Upper row shows PD-L1 immunohistochemistry staining, and lower row exhibits PD-L1 markup illustrating the different staining intensities.

tissue area analyzed (μm^2), biomarker area (μm^2), biomarker weak, moderate, and strong area (μm^2), percentage of biomarker positive tissue, percentage of biomarker weak, moderate, and strong positive tissue, biomarker average positive optical density, percentage of negative tissue and H-score.

Correlation between scores obtained by RNAscope and IHC were positive for all of them. However, for *CTLA4* the correlation was low (r=0.2512) and did not reach statistical significance (**Figure 3).**

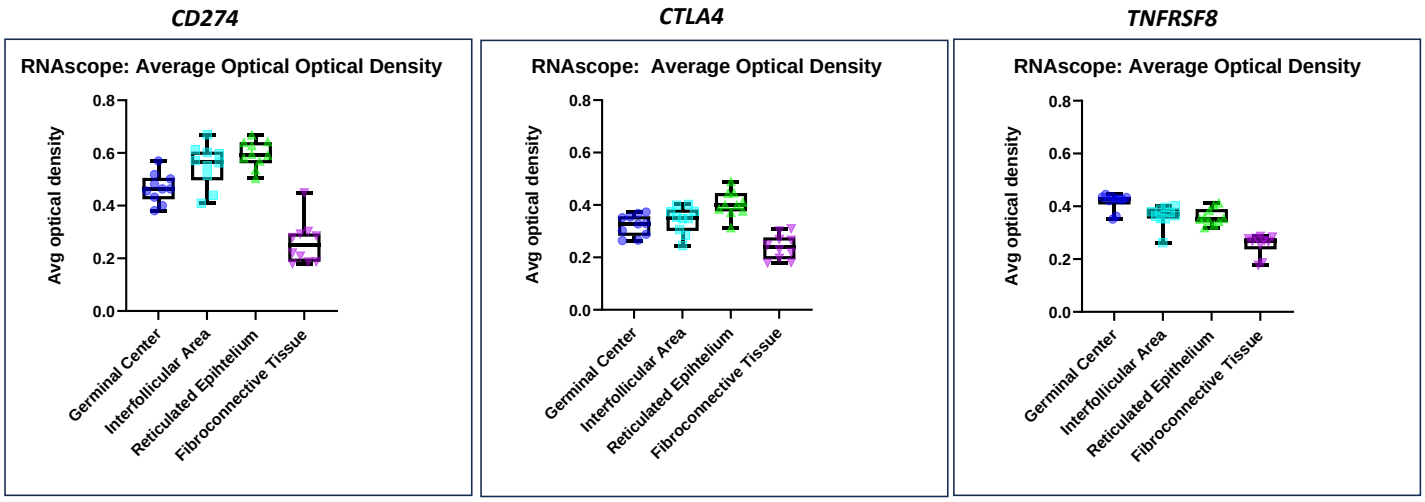

Figure 2. RNAscope signals of *CD274, CTLA4* and *TNFRSF8* target probes measured by Average Optical Densities by region of interest in different compartments of tonsil tissue.

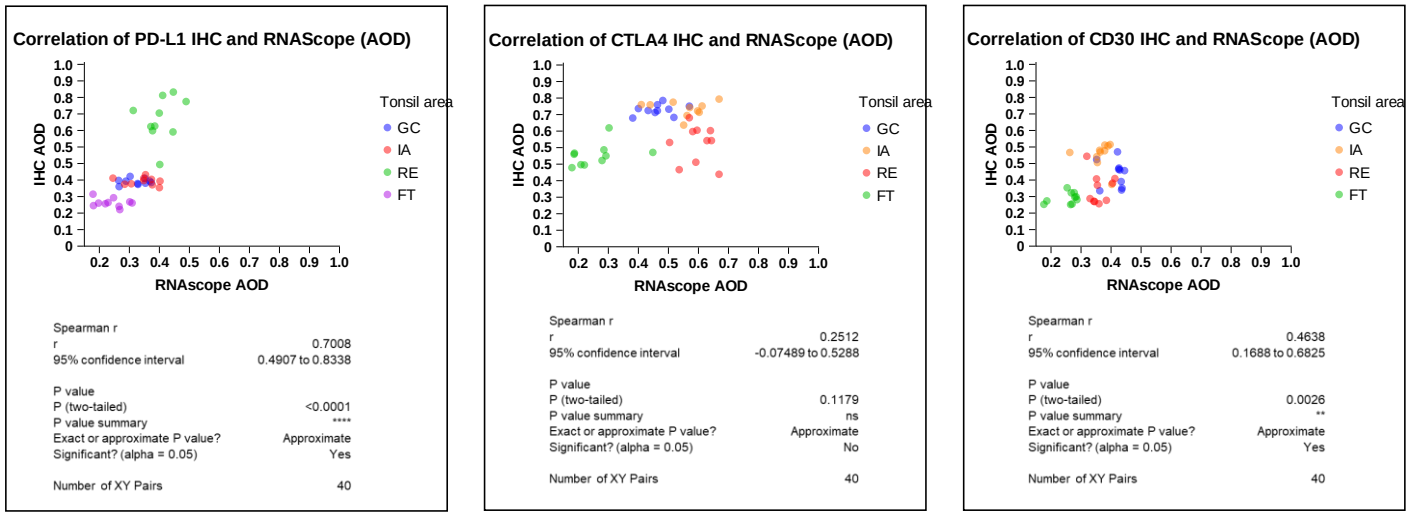

GC= Germinal Center, IA=Interfollicular Area, RE=Reticulated Epithelium, FT= Fibroconnective Tissue

Figure 3. Correlation plots between average optical density (AOD) for both Immunohistochemistry and RNAscope signals of *CD274* (PD-L1*), CTLA4*, and *TNFRSF8* (CD30) in different compartments of tonsil tissue.

Table 7. Descriptive statistics of average positive optical density of *CD274, CTLA4, TNFRSF8, IFNG, and IL-10* target probes stained with RNAScope assay by biological compartment of tonsil tissue.

Probe	Germinal Center	Interfollicular Area	Reticulated Epithelium	Fibroconnective Tissue
CD274				
Number of values	10	10	10	10
Minimum	0.2642	0.2453	0.3129	0.1788
25% Percentile	0.2826	0.3009	0.3757	0.193
Median	0.3282	0.351	0.4004	0.2381
75% Percentile	0.357	0.3822	0.4455	0.2764
Maximum	0.3728	0.4021	0.4889	0.3092
Range	0.1086	0.1567	0.1761	0.1304
Mean	0.3223	0.3437	0.4038	0.2397
Std. Deviation	0.04031	0.05083	0.04859	0.04677
Std. Error of Mean	0.01275	0.01607	0.01537	0.01479
CTLA4				
Number of values	10	10	10	10
Minimum	0.3813	0.4098	0.504	0.1788
25% Percentile	0.4244	0.4966	0.5612	0.1868
Median	0.4635	0.5665	0.5933	0.2496
75% Percentile	0.5056	0.605	0.6408	0.2946
Maximum	0.5697	0.6687	0.6686	0.4482
Range	0.1884	0.259	0.1646	0.2694
Mean	0.4667	0.553	0.5957	0.2588
Std. Deviation	0.05552	0.07927	0.05111	0.08219
Std. Error of Mean	0.01756	0.02507	0.01616	0.02599
TNFRSF8				
Number of values	10	10	10	10
Minimum	0.352	0.2625	0.3193	0.1763
25% Percentile	0.4067	0.3539	0.3394	0.2369
Median	0.4278	0.3713	0.353	0.2688
75% Percentile	0.4353	0.3916	0.3896	0.2803
Maximum	0.4449	0.4023	0.4128	0.2863
Range	0.0929	0.1398	0.09345	0.11
Mean	0.4167	0.3642	0.3605	0.2545
Std. Deviation	0.03214	0.0397	0.03088	0.03987
Std. Error of Mean	0.01016	0.01255	0.009766	0.01261
IFNG				
Number of values	10	10	10	10
Minimum	0.2038	0.1877	0.2305	0.1495
25% Percentile	0.2362	0.2175	0.2954	0.2066
Median	0.3412	0.2871	0.3486	0.2292
75% Percentile	0.4892	0.4003	0.4172	0.2705
Maximum	0.511	0.5171	0.4722	0.3587
Range	0.3072	0.3295	0.2416	0.2092
Mean	0.3519	0.3079	0.3543	0.2423
Std. Deviation	0.1217	0.1045	0.07529	0.06093
Std. Error of Mean	0.03848	0.03304	0.02381	0.01927
IL-10				
Number of values	10	10	10	10
Minimum	0.41	0.4042	0.3811	0.2175
25% Percentile	0.4196	0.4274	0.4818	0.2287
Median	0.4597	0.4668	0.5026	0.2843
75% Percentile	0.497	0.6042	0.6099	0.322
Maximum	0.5866	0.6929	0.7096	0.3287
Range	0.1766	0.2887	0.3285	0.1112
Mean	0.4678	0.5048	0.5383	0.2768
Std. Deviation	0.05869	0.1077	0.1022	0.04781
Std. Error of Mean	0.01856	0.03406	0.03233	0.01512

7. Analytical sensitivity and specificity

Analytical sensitivity was measured by the capacity of the assay to identify true positive or true negative expression as defined by gene amplification or by protein expression. We compared biomarker expression of a lung cancer TMA by RNAscope assay with the gene copy number by FISH and with the protein expression by standard IHC.

We tested RNAscope staining in a TMA section that have annotated information of *CD274 (PD-L1)* gene copy number information (FISH) in malignant cells, and protein PD-L1 (IHC) reported as percentage of positive malignant cells. Using these gold standards, true positive was defined as a tumor with C*D274* gene amplification (≥6 gene copy number in malignant cells) or protein PD-L1 expression of ≥1% in malignant cells; *CD274* positive by RNAscope was defined as >10 H-score (at least 10% of malignant cells with >=1 dot per cell). Using *CD274* gene amplification as gold standard, we found that the assay has a specificity of 68% and a sensitivity of 81% **Table 8**. Using protein PD-L1 IHC assay as gold standard the assay has a specific of 77% and sensitivity of 73% **Table 9**. In addition, PD-L1 protein expression and *CD274* gene copy numbers (FISH) positively correlated with *CD274* RNAscope H-score (r>4 and p value <0.0001) **Figure 4.**

Table 8. Assessment of the analytical specificity and sensitivity of RNAscope assay *for CD274* probe in lung cancer samples placed in a Tissue microarray using gene copy number (Fluorescence *in situ* hybridization) information to define true positive and negative expression.

PD-L1	FISH Positive	FISH Negative	Specificity	Sensitivity
RNAscope Positive	18	54	68	81
RNAscope Negative	4	117		

Table 9. Assessment of the analytical specificity and sensitivity of RNAscope assay *for CD274* probe in lung cancer samples placed in a Tissue microarray using protein (immunohistochemistry) information to define true positive and negative expression.

PD-L1	IHC Positive	IHC Negative	Specificity	Sensitivity
RNAscope Positive	42	30	77%	73%
RNAscope Negative	15	106		

8. Inter-run and intra-run reproducibility

To assess the reproducibility of the RNAscope assay, *TNFRSF8* target probe was evaluated in serial sections of a tonsil tissue (T51-2). Test 1 was performed in Day 1, while Test 2.1 and Test 2.2 was performed in Day 7 in the same run (inter and intra-run tests). Standard bright microscope and digital image analysis was used for the evaluation of RNAscope signals **Table 3 and Figure 5**.

For the quantitative digital image analysis, the regions of interest (10 GC, 10 IA, 10 RE and 10 FT) were evaluated to match the same regions in all tonsil tissue serial section **Figure 5.** Using the ISH v4.1.3 algorithm in HALO Software, a probe markup was established to identify and quantify the target probe in the selected ROIs **Figure 5.** Each biological compartment was analyzed. The AOD of RNAscope signals in all the selected biological

compartments was used to correlate the reproducibility of *TNFRSF8* target probe signals in inter and intra-run tests. We found a positive correlation between the tests in both the inter and intra runs, with a Spearman test that showed a rho >7 in all the tests and a *P* value <0.0001 **Figure 6.**

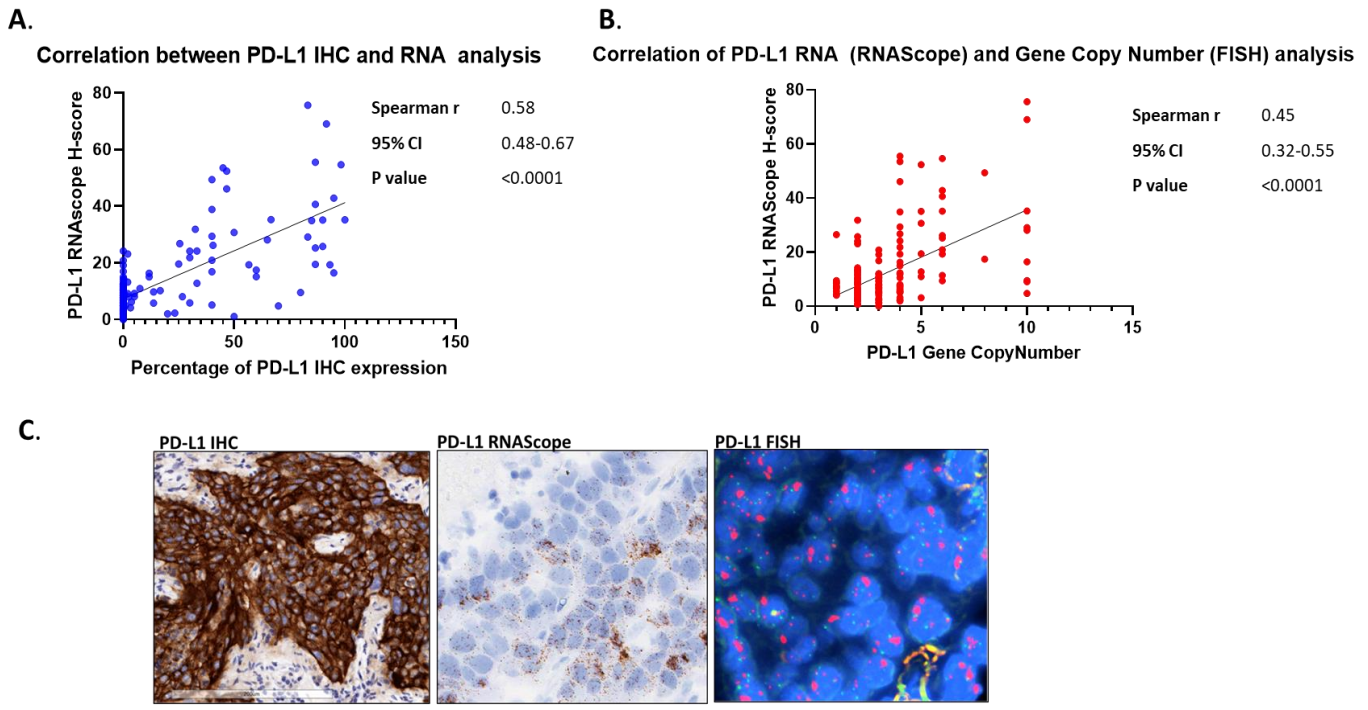

Figure 4. Concordance study between *CD274* gene expression by RNAScope with PD-L1 Immunohistochemistry (IHC) expression, and *CD274* gene copy number obtained by fluorescence *in situ* hybridization (FISH) in non-small cell lung carcinoma samples placed in a tissue microarray. **A and B** displays correlation plot between *CD274* (PD-L1) gene expression obtained by RNAScope assay and reported as H-score in malignant cells with PD-L1 protein IHC expression reported as percentage of positive expression in malignant cells **(A),** and *CD274* (PD-L1) gene copy number obtained by FISH **(B)** in non-small cell lung carcinoma samples. **C** shows microphotographs of a non-small cell lung carcinoma sample stained with *PD-L1* immunohistochemistry (left), RNAScope for *CD274* (PD-L1) (center) and FISH for *CD274 (*right)

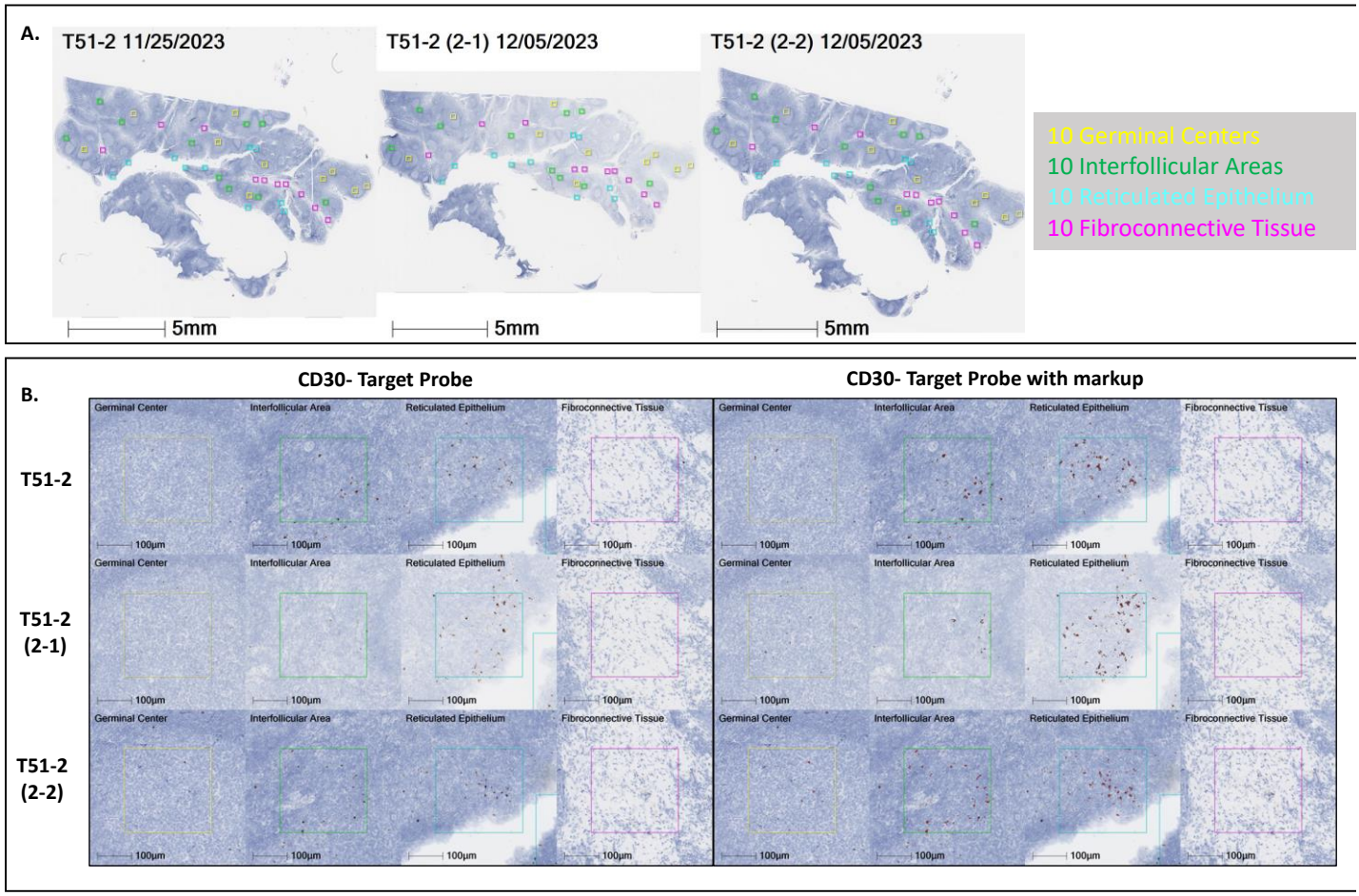

Figure 5. Inter and intra-run test for *TNFRSF8* RNAscope assay in tonsil tissue. **A).** Regions of interest selected for RNAscope evaluation in the same tonsil tissue in different tests at different days. **B).** Microphotographs at 20x magnification of tonsil tissue biological compartments showing TNFRSF8 target probe markup.

9. Conclusion

In conclusion, our data indicates that RNAscope assay for immune related targets shows a pattern of expression that matches the expected biological pattern and IHC expression patterns observed in reactive tonsil tissue controls. Gene expression of *CD274* positively correlated with protein expression by single IHC, and gene copy number at high specificity and sensitivity. We also observed high inter and intra-run reproducibility of the assay.

Of note, using single chromogenic RNAscope assay, the morphological evaluation of different cells within the immune cell-enriched areas of a tonsil was challenging due to the morphological changes caused by the assay which were not overcome by using different pretreatment conditions. Morphological features were better preserved in lung cancer tissue. We also did not observe a significant difference in expression among immune-enriched biological compartments, for example we expected to have higher expression of *CD274* in germinal center compared to interfollicular area, however our data revealed no significant differences between these compartments. In addition, in lung cancer, we observed false positive and false negatives samples when using protein or gene copy number gold standard assays, which may be due to post-translational modifications or

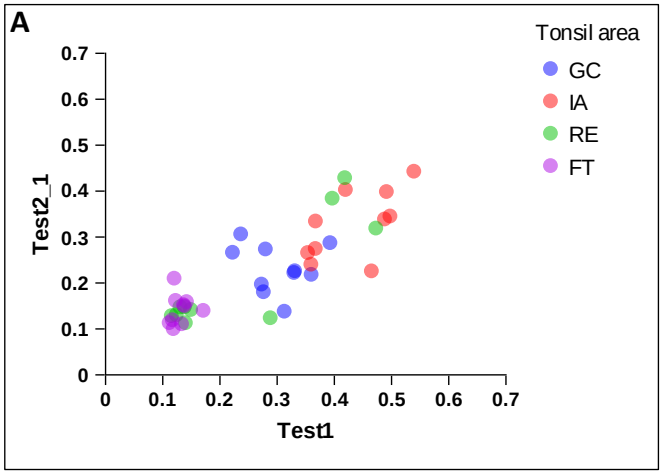

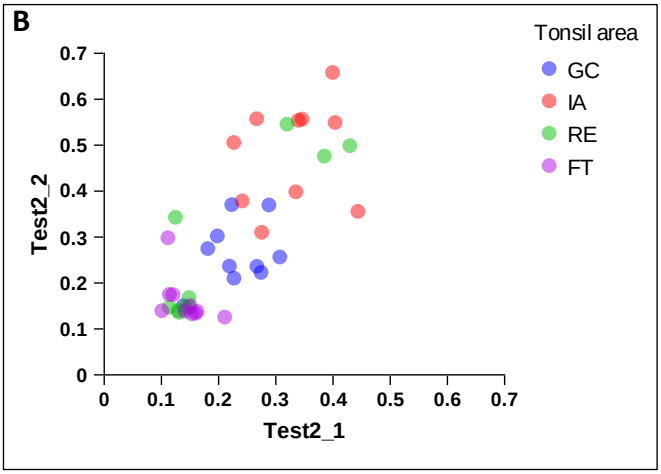

GC= Germinal Center, IA=Interfollicular Area, RE=Reticulated Epithelium, FT= Fibroconnective Tissue

C

Correlation Spearman r	Test1	Test2_1	Test2_2
Test1	1.00	0.84	0.84
Test2_1	0.84	1.00	0.71
Test2_2	0.84	0.71	1.00

Correlation Sample Size	Test1	Test2_1	Test2_2
Test1	40	40	40
Test2_1	40	40	40
Test2_2	40	40	40

95% Confidence Interval	Test1	Test2_1	Test2_2
Test1		0.7041 to 0.9119	0.7120 to 0.9146
Test2_1	0.7041 to 0.9119		0.5045 to 0.8393
Test2_2	0.7120 to 0.9146	0.5045 to 0.8393	

Correlation P values	Test1	Test2_1	Test2_2
Test1		<0.0001	<0.0001
Test2_1	<0.0001		<0.0001
Test2_2	<0.0001	<0.0001	

Figure 6. Correlation plots showing inter **(A)** and intra-assay **(B)** correlation between average optical densities of *TNFRSF8* RNAscope target probe in 3 tonsil tissue sections stained in **1.** Day 1 (Test 1); **2.** Day 7 (Test 2_1); and **3.** Day 7 (Test 2_2). Test 2_1 and Test2_2 were stained in the same run. **C.** Tables showing Spearman r, *P* values, sample size and 95% confidence interval values.

different biomarker expression in consecutive sections with tissue heterogeneity. Also, the RNAscope assay has limitations to perform distinct cell segmentation due to the morphological changes stated above.

Our data indicates that RNAscope assays are suitable alternative to investigate biomarkers that do not have robust options for IHC, such as cytokines which have low sensitivity of detection by standard IHC assay. RNAscope assays can also be used to visualize and quantify CAR/TCR vectors, microbiome, or other targets of interest. Customs probes can be designed by vendor (ACDbio) which offers an appealing approach to study any sequence target of interest.

10. References

1. Wang F, Flanagan J, Su N, Wang LC, Bui S, Nielson A, et al. RNAscope: a novel in situ RNA analysis platform for formalin-fixed, paraffin-embedded tissues. J Mol Diagn. 2012;14(1):22-9.

2. ACDbio. RNAscope® 2.5 LSx Reagent Kit – BROWN User Manual for BDZ 15/BXD 15 2018 [Available from: https://acdbio.com/sites/default/files/322700-USM%20RNAscope%20LSx%20BROWN%2005102018.pdf.

3. Lyford-Pike S, Peng S, Young GD, Taube JM, Westra WH, Akpeng B, et al. Evidence for a role of the PD-1:PD-L1 pathway in immune resistance of HPV-associated head and neck squamous cell carcinoma. Cancer Res. 2013;73(6):1733-41.

4. Qin W, Hu L, Zhang X, Jiang S, Li J, Zhang Z, Wang X. The Diverse Function of PD-1/PD-L Pathway Beyond Cancer. Front Immunol. 2019;10:2298.
5. Parra ER, Behrens C, Rodriguez-Canales J, Lin H, Mino B, Blando J, et al. Image Analysis-based Assessment of PD-L1 and Tumor-Associated Immune Cells Density Supports Distinct Intratumoral Microenvironment Groups in Non-small Cell Lung Carcinoma Patients. Clin Cancer Res. 2016;22(24):6278-89.
6. van der Weyden CA, Pileri SA, Feldman AL, Whisstock J, Prince HM. Understanding CD30 biology and therapeutic targeting: a historical perspective providing insight into future directions. Blood Cancer Journal. 2017;7(9):e603-e.
7. Marques-Piubelli ML, Kim DH, Medeiros LJ, Lu W, Khan K, Gomez-Bolanos LI, et al. CD30 expression is frequently decreased in relapsed classic Hodgkin lymphoma after anti-CD30 CAR T-cell therapy. Histopathology. 2023;83(1):143-8.

Immunohistochemistry and Digital Pathology Laboratory

RNAScope scientist leads:

Lorena Isabel Gomez, MD, Research Scientist

Wei Lu, MD, PhD, Principal Research scientist.

Director: Luisa Maren Solis Soto, MD, Associate Professor, MD Anderson Cancer Center

Signature (Luisa M. Solis Soto) **Date: 02/01/2024**